Journal of Cerebral Blood Flow & Metabolism (2011) 31, 504–513
© 2011 ISCBFM All rights reserved 0271-678X/11 $32.00
www.jcbfm.com

Impact of genetic and renovascular chronic arterial hypertension on the acute spatiotemporal evolution of the ischemic penumbra: a sequential study with MRI in the rat

Annelise Letourneur, Simon Roussel, Jérôme Toutain, Myriam Bernaudin and Omar Touzani

CERVOxy team 'Hypoxia and Cerebrovascular Pathophysiology', UMR CI-NAPS 6232, CNRS; CEA; Université de Caen Basse-Normandie; Université Paris Descartes, Centre CYCERON, Bd Henri Becquerel, CAEN cedex, France

Although chronic arterial hypertension (CAH) increases the risk of stroke and the severity of the resultant lesion, it is rarely integrated in preclinical studies. Here, we analyzed the impact of CAH on the acute spatiotemporal evolution of the ischemic penumbra as defined by the perfusion-weighted imaging/diffusion-weighted imaging mismatch. Sequential 7T-MRI examinations were performed from 30 minutes up to 4 hours after permanent cerebral ischemia in genetically hypertensive rats (spontaneously hypertensive rats, SHR), renovascular-hypertensive rats (RH-WKY), and their normotensive controls (Wistar-Kyoto rats, WKY). The apparent diffusion coefficient (ADC)-defined lesion was larger in hypertensive rats than in normotensive animals as early as 30 minutes after the ischemia. The ischemic penumbra was smaller in both genetically and renovascular-hypertensive rats (at 30 minutes; SHR = 66 ± 25 mm³, RH-WKY = 55 ± 17 mm³ versus WKY = 117 ± 14 mm³; $P < 0.008$) and there was no significant difference between the perfusion deficit and ADC lesion (mismatch definition of penumbra) as early as 90 minutes after the occlusion. Genetic hypertension and induced renovascular hypertension resulted in larger lesion and smaller penumbra that vanished rapidly. These data support the need to integrate CAH in preclinical studies relative to the treatment of stroke, as failure to do so may lead to preclinical results nonpredictive of clinical trials, which include hypertensive patients.
Journal of Cerebral Blood Flow & Metabolism (2011) **31,** 504–513; doi:10.1038/jcbfm.2010.118; published online 21 July 2010

Keywords: arterial hypertension; ischemic penumbra; MRI; perfusion–diffusion mismatch; preclinical model; stroke

Introduction

The global burden of stroke is a major health issue because of its incidence and its morbid consequences. Even if many pharmacological treatments of ischemic stroke have been proven efficient in animal studies, none could be transferred to the clinical situation with the same efficiency (O'Collins *et al*, 2006). One of the issues that has been put forward to explain this failure of translation of the bench results to the bed side is the inadequacy of the animal models of stroke (Durukan *et al*, 2008). Indeed, most of the available preclinical studies rely on the use of young and healthy animals devoid of concomitant pathologies such as chronic arterial hypertension (CAH), which is often associated with stroke in humans (Lawes *et al*, 2008).

The CAH is a frequent pathology with >25% of the worldwide population hypertensive and the incidence of this disease still increasing (29% predicted by 2025) (Kearney *et al*, 2005). The CAH is the major risk factor for stroke as >50% of strokes are attributable to high blood pressure and more than two thirds of patients suffering from stroke are hypertensive. Lowering blood pressure reduces stroke incidence; however, even if antihypertensive treatments are widely available, efficient control of hypertension is poorly achieved in the adult popula-

Correspondence: Dr O Touzani, CERVOxy team 'Hypoxia and Cerebrovascular Pathophysiology', UMR CI-NAPS 6232, Centre CYCERON, Bd Henri Becquerel, BP5229, 14074 CAEN cedex, France.
E-mail: touzani@cyceron.fr
This study was supported by the French Centre National de la Recherche Scientifique (CNRS) and the Conseil Régional de Basse-Normandie.
Received 17 March 2010; revised 24 June 2010; accepted 25 June 2010; published online 21 July 2010

tion. Furthermore, CAH is also an aggravating factor of the ischemic lesion (Takaba *et al*, 2004). Indeed, it is well known that this insidious pathology alters the structure and the function of cerebral arteries, which renders the brain more susceptible to severe diminution of arterial perfusion pressure (Iadecola and Davisson, 2008). Despite these facts, few experimental studies of ischemic stroke pathophysiology and treatment take CAH into account.

The influence of CAH on the ischemic penumbra, a brain region that represents the target of any acute therapeutic intervention, and on its kinetics, which by definition, determines the window of therapeutic opportunity has not been fully characterized. On the basis of perfusion-weighted imaging (PWI) and diffusion-weighted imaging (DWI), the ischemic penumbra is now widely defined as the mismatch between the volume of perfusion deficit and the volume of tissue with decreased diffusion of water molecules (Schlaug *et al*, 1999; Lövblad *et al*, 2003). Although this index has been criticized as perfusion deficit may encompass both penumbral and oligemic tissues (Sobesky *et al*, 2005; Takasawa *et al*, 2008), PWI/DWI mismatch provides an interesting approximation of the ischemic penumbra and has a major clinical application in the identification of patients able to respond to acute treatment (Olivot and Marks, 2008; Albers *et al*, 2006).

On the basis of the mismatch between PWI and DWI magnetic resonance imaging (MRI), we sought to further characterize the impact of CAH on the acute spatiotemporal evolution of the ischemic penumbra through the use of two well-characterized models of rat CAH (e.g., genetic and renovascular-induced hypertension compared with normotensive controls).

Materials and methods

Animals

Genetic-hypertensive rats (spontaneously hypertensive rats, SHR) and normotensive rats (WKY rats) were purchased from the R Janvier Breeding center, le Genest Saint-Isle, France. All rats were housed in a temperature-controlled room with 12 hours day/night cycle with food and water access *ad libidum*. The experimental procedure was approved by the Regional Ethic Committee for animal research (CEEAN 1106-21). Three groups of male rats were used: genetic-hypertensive rats (SHR, $n=11$); renovascular-hypertensive rats (Wistar-Kyoto (WKY) renovascular-hypertensive rats; RH-WKY, $n=10$) and their control, the normotensive rats (WKY, $n=10$). All the experiments were performed randomly and the data were analyzed in a masked manner.

Two-Kidney One-Clip Renovascular Hypertension

To induce renovascular hypertension, 10 5-week-old WKY rats underwent renal artery constriction according to the two-kidney one-clip model (Del Bigio *et al*, 1999). Rats were anesthetized with isoflurane (2% to 3% in 70/30 N_2O/O_2) and a median longitudinal incision was performed on the abdominal skin and muscle. Then, the left kidney was exposed, the renal artery and vein were isolated and a silver clip with an inner diameter of 0.20 mm was placed around the renal artery to induce stenosis. Abdominal muscle and skin were sutured, and the rats received an analgesic (Tolfédine 4%, 4 mg/kg intramuscularly) and thereafter were allowed to recover from anesthesia. Two rats died $\sim$2 months after the surgery probably because of renal insufficiency. The surviving rats were subjected to focal ischemia 3 months after the induction of renal artery stenosis.

Blood Pressure Measurements in Awake Animals

Arterial blood pressure (ABP) was measured in awake RH-WKY rats by the tail-cuff method (storage pressure meter-5002 Letica, Barcelona, Spain) before and fortnightly over the 3 months after stenosis. In SHR and WKY, ABP was measured weekly during the month preceding the induction of ischemia. To ensure correct ABP assessments, rats were prewarmed at 35°C and the measures were repeated five times for each session.

Cerebral Ischemia

The SHR, WKY, and RH-WKY rats were anesthetized with isoflurane (1.9% to 2.3%) and were intubated and artificially ventilated (Rodent Ventilation-683 Harvard, Holliston, MA, USA). End tidal CO_2 was continuously measured (Micro-capnograph CI240 Colombus Instruments, Columbus, OH, USA) and corrected if necessary. Polyethylene tubings were inserted into the femoral vein for injections and into the femoral artery for monitoring of ABP, heart rate and to withdraw samples of arterial blood. Blood samples were taken once before ischemia and three times during MRI acquisitions, to measure blood gases, pH, and base deficit (Bayer-860, Bohemia, NY, USA). Rectal temperature was monitored and maintained around 37.5°C, with a thermostatically controlled heating pad (Homeothermic Blanket, Harvard, Holliston, MA, USA) during the whole period of anesthesia.

Permanent focal cerebral ischemia was induced using the intraluminal approach (Lecrux *et al*, 2007). The rat was placed into a stereotaxic frame (Kopf Instruments, Tujunga, CA, USA) and a laser-Doppler flowmetry probe (FloLab Moor Instruments, Millwey, UK) was positioned on the right parietal bone, corresponding to the middle cerebral artery territory (coordinates 1.5 mm posterior, 5.5 mm lateral to the bregma), previously thinned by a saline-cooled dental drill. Then the animal was placed in the supine position and a 0.18-mm diameter nylon thread coated with a thermofusible glue to form a distal cylinder of 0.380 mm diameter and 2.5 mm length was introduced into the internal carotid, *via* the external carotid artery, and advanced until it occluded the middle cerebral artery. The flow within the common carotid artery was only interrupted at the time of the introduction of the thread. Focal ischemia induction was confirmed by the drop of relative cerebral blood flow as measured by laser-Doppler flowmetry (relative cerebral blood flow decrease in 5 minutes after

ischemia was 56% ± 13%, 62% ± 13%, and 67% ± 12%, respectively, in WKY, SHR, and RH-WKY). The rats were then transferred into the magnet.

Magnetic Resonance Imaging

The MRI was performed on a Bruker Pharmascan 7-Tesla horizontal magnet (Ettlingen, Germany). Rats were placed in a stereotaxic head holder in the magnet and physiologic parameters were monitored as described above. The animals underwent MRI acquisitions over the 4 hours after ischemia. For all imaging modalities, seven slices, 1.5 mm thick with a 0.5-mm interslice gap were acquired (except for angiography) with a $38.4 \times 38.4\,mm^2$ field of view (FOV) (except for angiography and T2* EPI). The DWI was acquired at 30, 90, 120, 150, 180, and 240 minutes after occlusion with the following parameters: two-shot spin echo echo-planar images, 128×128 matrix, TR/TE = 3500/41.04 milliseconds, *b*-values = 0, 1000 sec/mm^2, 30 directions. The whole of the sequence lasted 4 minutes and 5 seconds. Apparent diffusion coefficient (ADC) maps were calculated. The PWI was performed at 30, 150, and 240 minutes by an intravenous injection of a bolus of contrast agent (0.3 mL, intravenous at the 15th second of imaging, Gadolinium Dimeglumine Chelate, Magnevist, Bayer Santé, Loos, France). T2* EPI were acquired with 78×78 matrix, $23.4 \times 23.4\,mm^2$ FOV with saturation slice outside, $0.300 \times 0.300\,mm^2$/pixel resolution, TR/TE = 500/10.32 milliseconds and 120 repetitions. Time of flight angiography was acquired at 40 and 240 minutes after ischemia (3D FLASH; 32 slices, 0.175 mm thick, TR/TE = 10/1.81 milliseconds, flip angle = 20°). T1-enhancement imaging was acquired 5 minutes after each T2* EPI. The sequence parameters were as above: Fast T1-weighted (rapid acquisition with relaxation enhancement, RARE factor 4), 256×256 matrix, $0.150 \times 0.150\,mm^2$/pixel resolution, TR/TE = 1300/7.334 milliseconds. A T2* image (FLASH); 256×256 matrix, $0.150 \times 0.150\,mm^2$/pixel resolution; TR/TE = 400/11 milliseconds. This sequence, performed at the beginning and the end of the experiment, was to verify the absence of intracerebral hemorrhage.

At the end of MRI acquisitions, the catheters were removed and the skin sutured, local anesthetic was applied to surgical wounds and the rats were allowed to recover from anesthesia.

Post Mortem Evaluation

The animals were euthanized 24 hours after ischemia. Coronal brain slices (20 μm) were cryostat-cut and stained with thionin. The stained sections were then photographed and infarct volumes were calculated, with oedema correction according to the following equation: infarct volume = contralateral hemisphere volume minus ipsilateral noninfarcted tissue volume (Lin *et al*, 1993).

Data Analysis

The MR images were analyzed in a masked manner using the image processing Paravision and in-house macros using ImageJ software. For all MRI modalities, the images were analyzed through the use of normalized thresholds to take into account any interindividual or global time-related variation of the parameter analyzed. This approach also allows each animal to be used as its own control at all time points. Abnormal ADC was defined by thresholding the images at the mean minus 2 s.d. of the values of the contralateral (nonischemic) hemisphere with the exclusion of the ventricles. Regarding the PWI, time to peak and maximal signal drop maps were calculated from the first pass of gadolinium chelate information. The time to peak is calculated as the time taken for the curve to peak from the last baseline period. The maximal signal drop illustrates the degree of signal drop and infers severely hypoperfused pixels. Pixels were considered abnormally perfused when either the time to peak was longer than that of the contralateral tissue plus 2 s.d. or when the maximal signal drop was < 3 s.d. of the basal signal. The volume of PWI–DWI mismatch was calculated by subtracting the volume of tissue with significant reduction in ADC from that with significant perfusion deficit. Given the kinetics of gadolinium chelate in the plasma, the PWI acquired at 30, 150, and 240 minutes were used to calculate the mismatch at 30 and 90 minutes, 120 and 150 minutes, and 180 and 240 minutes, respectively.

Incidence maps of the ADC-defined lesion and the hypoperfused area were generated. Images were first coregistered based on the ImageJ plugin turboReg (Thévenaz *et al*, 1998). The coregistration was performed on masks of the whole brain and then applied to both the lesion masks and the ADC maps. The incidence map was generated by summing all lesion masks from the same slice and applying a color look-up table. This map was then overlayed on averaged coregistered ADC maps. The same procedure was performed to generate hypoperfusion incidence maps. Furthermore and to illustrate the mismatch, DWI were resized and coregistered to PWI.

Statistical Analyses

Data are represented as mean ± s.e.m. Statistical analysis was performed with analysis of variance (ANOVA) or two-way repeated measures ANOVA followed, where appropriate, by Fisher's protected least significant difference or by paired *t*-test with Bonferroni correction.

Results

Physiologic Parameters

In RH-WKY, ABP was similar to those of WKY before the induction of renal artery stenosis and then increased progressively to reach a plateau 4 weeks later, corresponding to an increase of 30%. At this time, ABP was similar in awake SHR and RH-WKY but significantly higher than that measured in awake WKY ($P < 0.0001$) (Figure 1A). During the induction of ischemia and MRI acquisitions, arterial pressure remained stable and significantly higher in SHR and RH-WKY compared with WKY ($P < 0.001$)

(Figure 1B). The $PaCO_2$, PaO_2, blood pH, body temperature, and heart rate were in normal range and similar between all groups of animals (Table 1). All animals survived the whole period of MRI acquisition and recovered from anesthesia. Unfortunately two animals (one WKY and one RH-WKY) were discarded from subsequent analyses because of technical failures during the MRI acquisitions. The final number of rats included was the following: WKY, $n = 9$ (308 ± 7 g, 14 ± 1 weeks old); SHR, $n = 11$ (306 ± 9 g, 14 ± 1 weeks old), and RH-WKY, $n = 7$ (348 ± 29 g, 17 ± 1 weeks old).

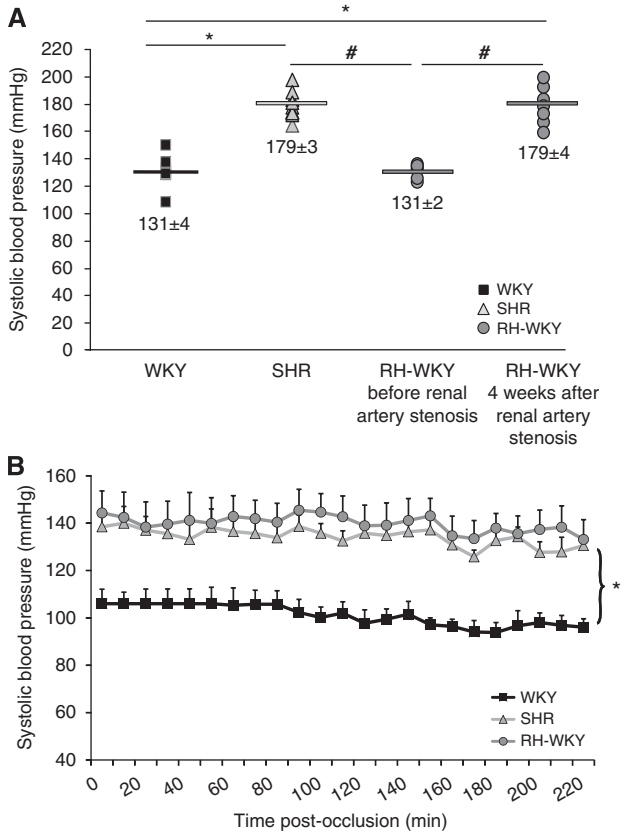

Figure 1 (**A**) Noninvasive measurement of systolic arterial pressure (SBP) in awake rats before the induction of ischemia. ■ WKY ($n = 9$); △ SHR ($n = 11$); ● RH-WKY before and after renal artery stenosis ($n = 7$). Fisher protected least significant difference following a significant analysis of variance (ANOVA): $^*P < 0.0001$ versus WKY; $^\#P < 0.0001$ versus RH-WKY before stenosis. (**B**) The SBP in anesthetized animals during MRI acquisitions. Fisher protected least significant difference following a significant repeated measures ANOVA: $^*P < 0.001$; SHR and RH-WKY versus WKY. RH-WKY, renovascular-hypertensive WKY; SHR, spontaneously hypertensive rats; WKY, normotensive Wistar-Kyoto.

Magnetic Resonance Imaging Observations

The MR angiography performed at 30 minutes and 4 hours after ischemia confirmed the arterial occlusion and the absence of spontaneous reperfusion in all animals as illustrated by the disappearance of the right middle cerebral artery (Figure 2). The T1-enhancement and T2* imaging did not reveal, respectively, any leak of the gadolinium chelate in the parenchyma nor any intracerebral hemorrhage in all the animals irrespective of the group studied (Figure 2). However, ADC maps and perfusion images elicited well-delineated lesions at all times analyzed (Figure 2).

Evolution of Apparent Diffusion Coefficient-Defined Lesions

The mean ADC values in the contralateral hemisphere were similar between WKY, SHR, and RH-WKY and remained stable over time around $0.810 \pm 0.107 \times 10^{-3}$ mm^2/sec (mean ± s.d.). Indeed, when all the groups are taken together, the ADC values were: $0.815 \pm 0.05 \times 10^{-3}$; $0.814 \pm 0.06 \times 10^{-3}$; $0.818 \pm 0.06 \times 10^{-3}$; $0.813 \pm 0.05 \times 10^{-3}$; $0.806 \pm 0.06 \times 10^{-3}$; $0.803 \pm 0.07 \times 10^{-3}$ mm^2/sec, respectively, at 30, 90, 120, 150, 180, 240 minutes after occlusion. There was no significant time effect, which suggests no major effect of anesthesia. The normalized threshold calculated on each slice as the mean values of the contralateral hemisphere (excluding the ventricles) minus 2 s.d. was, on average, 0.6×10^{-3} mm^2/sec (26% ADC reduction) and remained stable at all the time points analyzed. In the lesion, as defined by these thresholds, the ADC was severely reduced from 30 minutes after

Table 1 Physiological parameters during the induction of ischemia and MRI acquisition

	$PaCO_2$ (mm Hg)	*PaO_2 (mm Hg)*	*pH*	*Temperature (°C)*	*Heart rate (min^{-1})*
Ischemia induction					
WKY	34.8 ± 4.2	126.62 ± 40.6	7.43 ± 0.04	37.3 ± 0.2	335 ± 52
SHR	31.7 ± 4.9	157.25 ± 29.4	7.5 ± 0.04	37.4 ± 0.1	311 ± 16
WKY-RH	32.9 ± 6.7	123.01 ± 19.9	7.5 ± 0.04	37.4 ± 0.4	292 ± 46
MRI acquisition					
WKY	34.8 ± 4.6	134.2 ± 25.6	7.43 ± 0.05	37.4 ± 0.2	333 ± 44
SHR	33.7 ± 5.8	144.2 ± 19.5	7.43 ± 0.03	37.5 ± 0.2	312 ± 26
WKY-RH	36.5 ± 4.7	139.2 ± 24.6	7.43 ± 0.02	37.4 ± 0.2	288 ± 47

MRI, magnetic resonance imaging; SHR, spontaneously hypertensive rats; WKY-RH, Wistar-Kyoto renovascular-hypertensive rats.

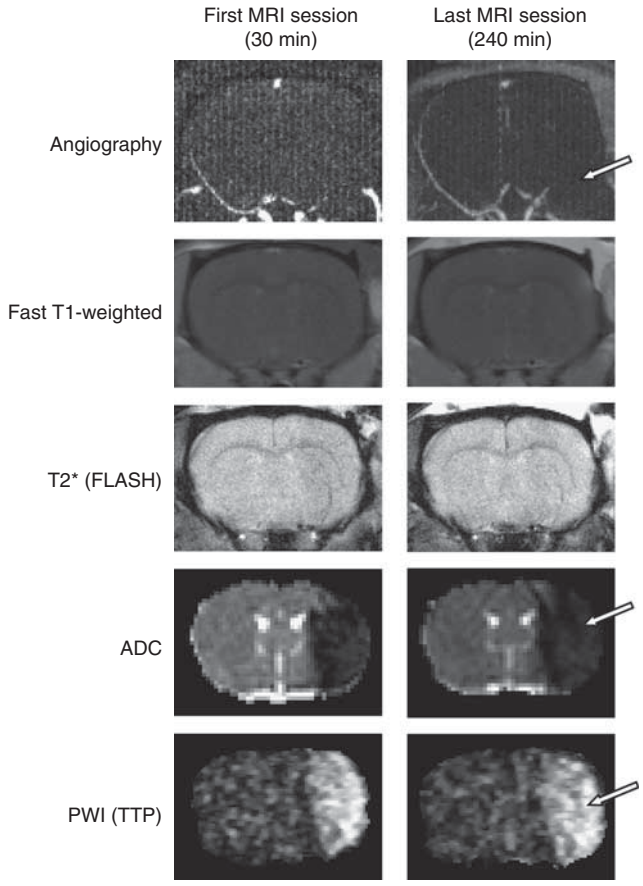

Figure 2 Representative images, at the first and the last examinations of magnetic resonance (MR) angiography, fast T1-weighted sequence, T2* fast low-angle-shot sequence, apparent diffusion coefficient (ADC) map, and perfusion-weighted imaging (PWI) (time to peak, TTP) in a spontaneously hypertensive rats (SHR) animal. The MR angiography revealed the persistence of middle cerebral artery (MCA) occlusion. Arrow indicates the disappearance of the left MCA, illustrating the absence of perfusion of this one. Fast T1-weighted sequence did not show any abnormality, which indicates the absence of blood–brain barrier breakdown. T2* (FLASH) sequence highlighted the absence of hemorrhage. ADC map revealed the presence of tissue with cytotoxic edema indicated by an area with drastic diminution of ADC values (cytotoxic edema is indicated by arrow). The TTP map extracted from the information provided by the first pass of gadolinium chelate showed the presence of hypoperfused tissue in all the animals as shown by an arrow on this image.

occlusion ($0.55 \pm 0.01 \times 10^{-3}$, $0.54 \pm 0.01 \times 10^{-3}$, and $0.53 \pm 0.02 \times 10^{-3}$ mm^2/sec in WKY, SHR, and RH-WKY, respectively). These values did not differ between the groups at any time point but gradually decreased over time (ANOVA repeated measures, time effect: $P < 0.0001$, no group effect, no interaction). At 4 hours after occlusion, ADC values within the lesion were, respectively, $0.50 \pm 0.02 \times 10^{-3}$, $0.48 \pm 0.01 \times 10^{-3}$, and $0.47 \pm 0.02 \times 10^{-3}$ mm^2/sec in WKY, SHR, and RH-WKY groups. These values illustrate that the severity of the cytotoxic edema increases as a function of time and in a similar way in all three groups.

The ADC-defined lesion was more extended, especially in the antero-posterior axis, in hypertensive compared with normotensive rats as early as 30 minutes after occlusion (Figure 3) (ADC-defined lesion volumes at 30 minutes after occlusion were: SHR = 132.7 ± 14.0 mm^3 and RH-WKY = 117.6 ± 9.7 mm^3 versus WKY = 76.1 ± 11.7 mm^3; $P < 0.05$) (Figure 4A). Quantification of the lesion volume at later times revealed that the ADC-defined lesion volume was larger in hypertensive rats (SHR and RH-WKY) compared with normotensive ones (WKY) at all the time points (Figure 4A). From 120 minutes after occlusion, the ADC-defined lesion was greater in SHR relative to RH-WKY ($P < 0.05$) (ADC-defined lesion volumes at 120 minutes after occlusion were: WKY = 98.4 ± 12.2 mm^3, SHR = 188.4 ± 14.2 mm^3, and RH-WKY = 148.1 ± 11.4 mm^3; $P < 0.03$) (Figure 4A). Regarding the temporal evolution, the ADC-defined lesion volume significantly increased in all three groups between 30 minutes and 4 hours after occlusion (30 minutes versus 4 hours after occlusion; $P < 0.0001$). However, the volume of the lesion at 90 minutes was significantly different from that measured at 30 minutes in SHR and RH-WKY ($P < 0.01$), but not in WKY. The volume of ADC-defined lesion at 4 hours after occlusion was highly correlated ($R^2 = 0.77$; $P < 0.001$), with the volume of lesion defined by histology at 24 hours (122.7 ± 26.5, 153.4 ± 14.4, 229.9 ± 18.0 mm^3 in WKY, RH-WKY, and SHR, respectively).

Evolution of Hypoperfused Tissue Volumes

All rats displayed a reduction of blood flow in the ipsilateral hemisphere (Figure 3B). The volume of hypoperfused tissue remained essentially stable over time after ischemia, although there was a tendency toward an increase in SHR (Figure 4B). At 30 minutes after occlusion, there was no difference in the volumes of hypoperfused tissue between groups (192.9 ± 17.0 mm^3, 198.8 ± 14.2 mm^3, 172.2 ± 13.8 mm^3, respectively, in WKY, SHR, and RH-WKY; $P > 0.24$). However, at 4 hours after occlusion, the hypoperfused tissue volume was greater in SHR compared with RH-WKY and WKY groups (218.3 ± 17.15 mm^3, 168.9 ± 12.5 mm^3, and 176.5 ± 12.3 mm^3, respectively, in SHR, RH-WKY, and WKY; $P < 0.04$) (Figure 4B).

Evolution of the Perfusion–Diffusion Mismatch

The perfusion–diffusion mismatch, operationally defined by a significant difference between ADC-defined lesion volume and hypoperfused tissue volume, was more extended in normotensive than in hypertensive animals (Figure 5). Quantification of the volume of the ischemic penumbra as a function of time indicated that in normotensive rats, the PWI/DWI mismatch was significant at all the time

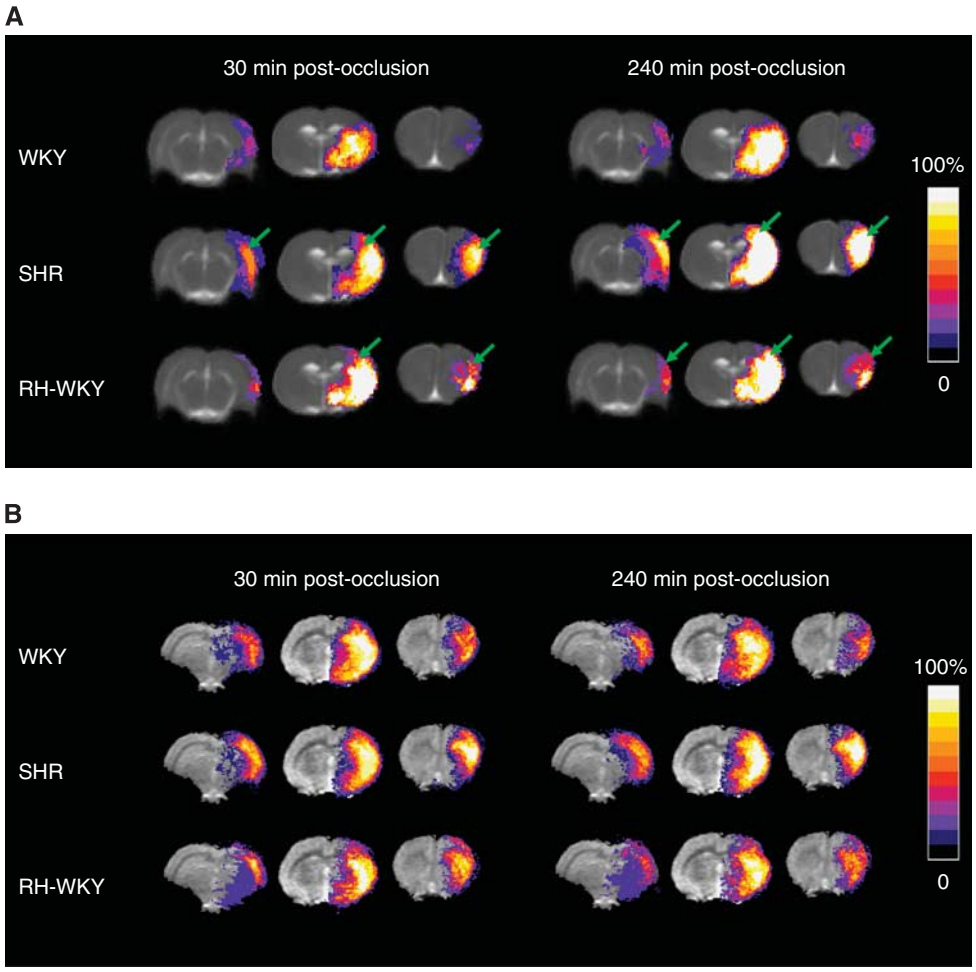

Figure 3 (**A**) Apparent diffusion coefficient (ADC)-defined lesions represented as incidence maps in WKY ($n = 9$), SHR ($n = 11$), and RH-WKY ($n = 7$) at 30 and 240 minutes after occlusion. At all times, lesions are larger in hypertensive than in normotensive rats involving an extended zone of the cortex and being more widespread in an antero-posterior direction (indicated by arrows). The ADC-defined lesions expand along time in the three groups. (**B**) Hypoperfusion represented as incidence maps at 30 and 240 minutes after occlusion. The color representations are shown according to the scale depicted on the right, in which black is without a lesion in any animal and white is where 100% of the animals displayed an abnormal signal. RH-WKY, renovascular-hypertensive WKY; SHR, spontaneously hypertensive rats; WKY, normotensive Wistar-Kyoto.

points although it gradually decreased with time. However, both in SHR and RH-WKY, the ischemic penumbra was significant only at 30 minutes after occlusion and decreased dramatically at 90 minutes and disappeared thereafter (mismatch perfusion–diffusion at 30 minutes after occlusion: SHR = $66.0 \pm 24.8\,mm^3$, RH-WKY = $54.6 \pm 17.1\,mm^3$, and WKY = $116.8 \pm 13.7\,mm^3$; $P < 0.0001$ (two-way ANOVA for each time (MRI measurements and groups); significant main MRI measurements effect: $P < 0.0001$ with no interaction, no group effect, at 30 minutes after occlusion). At 90 minutes, SHR = $23.6 \pm 13.3\,mm^3$, RH-WKY = $34.0 \pm 16.8\,mm^3$; $P < 0.04$ versus WKY = $92.9 \pm 15.3\,mm^3$; $P < 0.017$ (paired *t*-test with Bonferroni correction after significant two-way ANOVA for each time (MRI measurements and groups) (Figure 6). The ischemic penumbra was larger in WKY than in SHR and RH-WKY at all the times ($P < 0.008$ Fisher protected least significant difference for difference in mismatch volume between SHR and RH-WKY versus WKY following a significant ANOVA main group effect with no interaction). The quantification of the perfusion–diffusion mismatch on each slice indicated that the mismatch essentially vanished in the center of the middle cerebral artery territory in hypertensive rats relative to normotensive ones (Figure 5).

Discussion

Our present study shows that both genetic and renovascular CAH exacerbate the ischemic brain lesion and dramatically accelerate the evolution of the ischemic penumbra into an irreversible lesion. Our results imply that CAH considerably narrows the window of therapeutic opportunity and emphasize the importance of taking into account this

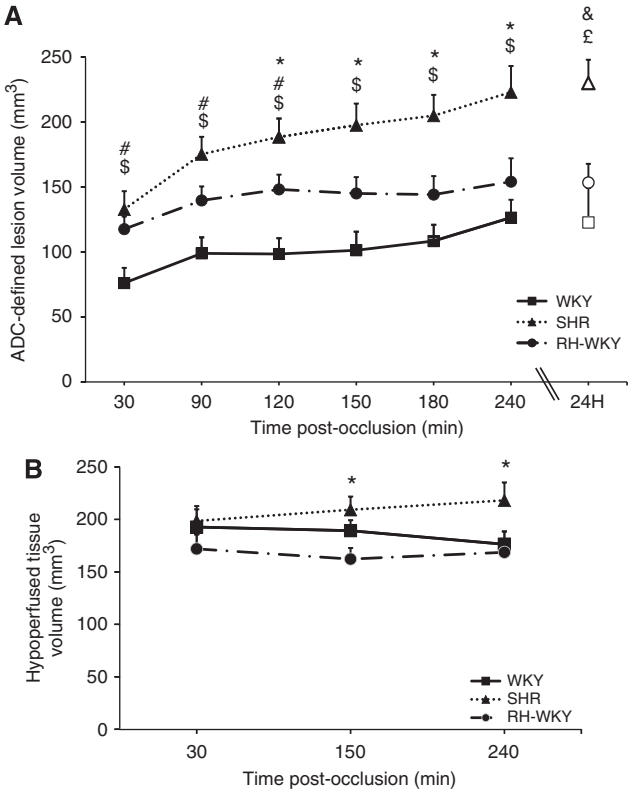

Figure 4 (**A**) Temporal evolution of the apparent diffusion coefficient (ADC)-defined lesion volume during the 4 hours after ischemia (filled symbols) and histologic infarct volume at 24 hours after occlusion (open symbols). $^{\$}P < 0.0001$ SHR ($n = 11$) versus WKY ($n = 9$); $^{*}P < 0.03$ SHR versus RH-WKY ($n = 7$); $^{\#}P < 0.05$ RH-WKY versus WKY (two-way repeated measures analysis of variance (ANOVA): Time × group interaction, $P < 0.04$, followed by ANOVA at each time and then a Fisher protected least significant difference). $^{\&}P < 0.002$ SHR versus WKY; $^{£}P < 0.03$ SHR versus RH-WKY (ANOVA followed by Fischer protected least significant difference). (**B**) Temporal evolution of the hypoperfused tissue volume: two-way repeated measures ANOVA indicated an interaction ($P = 0.08$); ANOVA at each time showed significance at the last two times; Fisher protected least significant difference at those times: $^{*}P < 0.04$ SHR versus RH-WKY. RH-WKY, renovascular-hypertensive WKY; SHR, spontaneously hypertensive rats; WKY, normotensive Wistar-Kyoto.

comorbid factor in preclinical investigations. Indeed, despite several recommendations from committees of experts regarding the preclinical development of stroke therapies, CAH is rarely considered in stroke models.

Recently, McCabe *et al* (2009) have reported a limited penumbra after focal ischemia in SHR-SP compared with normotensive rats. Nonetheless, SHR-SP are well known to exhibit an exacerbated ischemic lesion independent from arterial hypertension *per se* (Gratton *et al*, 1998). Accordingly, one question remains as to whether the accelerated disappearance of the penumbra in the SHR-SP is related to CAH or is merely due to intrinsic characteristics of this strain. In this study, based on MRI, we further analyzed this issue in two different models of hypertension: namely, genetic and induced hypertension. First, we directed our study toward SHR, the most common strain used in studies on essential arterial hypertension and their normotensive controls, the WKY. In SHR, and in accordance with the study of Legos *et al* (2008), ADC-defined lesions were greater than those of normotensive rats. Moreover, our study revealed that the ADC-defined lesion was greater even in the 30 minutes after occlusion in comparison to WKY (Figure 4A). At 4 hours, this ADC-defined lesion correlated with the volume of infarction quantified by histology at 24 hours. These data also support that the image analysis approach used in our study is relevant. Indeed, the aim of the study was not to define any absolute threshold but rather to use an objective method to delineate abnormal ADC values in which each animal constitutes its own control at each time. On the basis of this approach, our thresholds (on average a 26% reduction in ADC values) are consistent with those reported in the literature (Shen *et al*, 2003; McCabe *et al*, 2009). The same method of analysis was performed to examine the perfusion deficit based on the combination of two reliable parameters (maximal signal drop and time to peak delay) (Grandin *et al*, 2002).

To assess the distribution and characteristics of the ischemic penumbra, we relied on the concept of the PWI/DWI mismatch. Although the robustness of this concept has been criticized as perfusion deficit measured by MRI may encompass both penumbral and oligemic tissues and thus overestimate the penumbra, it is increasingly used in clinic to identify patients that may display salvageable ischemic tissue (Olivot and Marks, 2008). Perfusion deficit, in our study was measured, as generally performed in humans, by the analysis of the first pass of gadolinium chelate. This approach has been shown to provide equivalent information on the perfusion deficit as quantified through the use of continuous arterial spin labeling (Bråtane *et al*, 2010). The volume of initially hypoperfused tissue remained essentially stable over time after ischemia in normotensive animals (ANOVA repeated measures, time effect: $P = 0.44$) as has been previously described (Legos *et al*, 2008; Bardutzky *et al*, 2005). However in SHR, hypoperfusion expanded with time (ANOVA repeated measures, time effect: $P < 0.05$) and was greater than that of WKY at 240 minutes after the occlusion, suggesting a failure of collateral circulation in SHR. These data also concord with those reported by McCabe *et al* (2009) although in their study the perfusion deficit was limited to the analysis of on one brain slice and thus no volumetric information on hypoperfusion can be derived. Although the perfusion deficits were measured only at three time points (to enable clearance of the contrast agent between successive injections), our results show that the evolution of the volume of perfusion deficit is only moderate as compared with

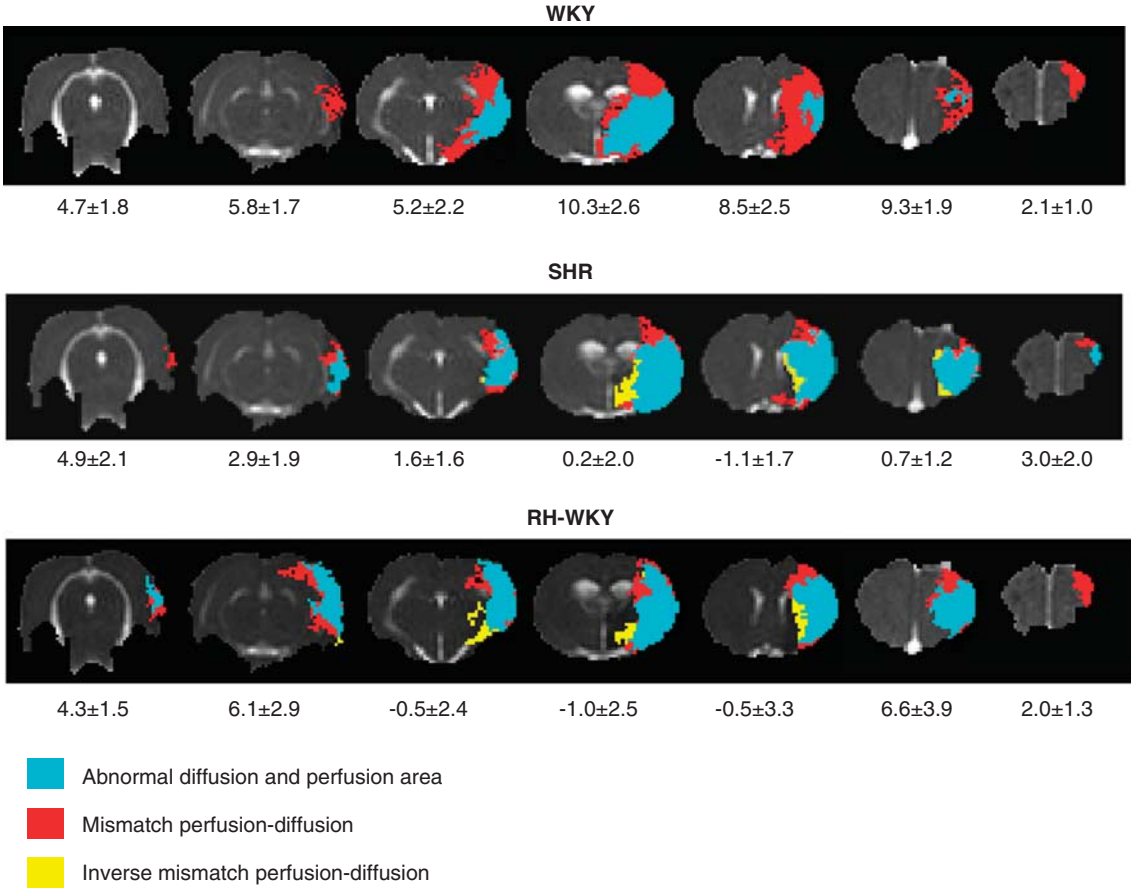

Figure 5 Representative perfusion–diffusion mismatch in a WKY, SHR, and RH-WKY rat at 90 minutes after occlusion. The blue color indicates abnormal diffusion area, whereas the red color indicates the ischemic penumbra as defined by perfusion–diffusion mismatch. The yellow color indicates the inverse mismatch corresponding to an area with reduced apparent diffusion coefficient (ADC) but normal perfusion. The mean area of the mismatch per group is indicated under each slice (mm^2). RH-WKY, renovascular-hypertensive WKY; SHR, spontaneously hypertensive rats; WKY, normotensive Wistar-Kyoto.

that of ADC, which justifies the use of only three time points of PWI to derive penumbra volumes at six time points. In this study, a significant difference between the perfusion deficit and ADC-defined lesion was present at all the time points in WKY animals although it progressively decreased with time. This profile of evolution is in agreement with that reported by Bardutzky *et al* (2005), highlighting the slow growth of the lesion in WKY, a rat strain known to display smaller and more variable brain ischemic lesions (Duverger and MacKenzie, 1988). In contrast, in SHR, the difference between the perfusion deficit and ADC-derived lesion was significant only at 30 minutes and almost completely disappeared at later time points (Figure 6).

The differences observed between SHR and WKY (strains with a similar genetic background) in the evolution of the ischemic penumbra could be explained by chronic hypertension-induced functional and structural alterations of the brain vasculature. Indeed, eutrophic and hypertrophic remodeling of the brain arteries and the shift of the autoregulation curve are well-known hallmarks of the vascular changes induced in SHR (Mulvany *et al*, 1978). Nonetheless, data exist in the literature, although to a lesser extent, relative to SHR-SP, to show that hypertension *per se* does not entirely underlie the sensitivity of SHR to cerebral ischemia (Lecrux *et al*, 2007). Indeed, we have previously shown that 7-week-old SHR, in which hypertension is not yet established, also exhibit exacerbated ischemic brain damage when compared with age-matched WKY (Lecrux *et al*, 2007). On the basis of these observations, we have used another well-characterized model of nongenetic hypertension, induced by renal artery stenosis in WKY (Del Bigio *et al*, 1999). In those animals, arterial pressure increased after stenosis and reached a plateau after 4 weeks. All the animals were subjected to ischemia 3 months after the induction of hypertension. At this time, it is known that hypertension induces structural (thickening of small artery walls, altered vasodilatation (Li *et al*, 1996; Del Bigio *et al*, 1999; Stankevicius *et al*, 2002)) and functional alterations of the cerebral circulation (e.g., shift of the lower limit of cerebral blood flow autoregulation) similar

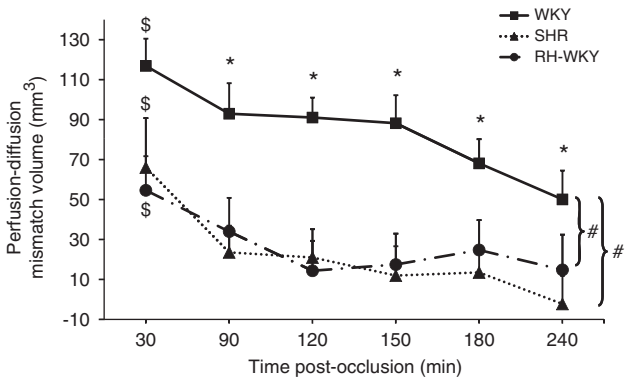

Figure 6 Evolution of the ischemic penumbra volume (perfusion–diffusion mismatch). $^{\$}P < 0.05$ for significant mismatch (i.e., significant difference between apparent diffusion coefficient (ADC) and hypoperfusion abnormality volumes at each time): two-way analysis of variance (ANOVA) for each time (magnetic resonance imaging (MRI) measurements and groups); significant main MRI measurements effect: $P < 0.0001$ with no interaction. $^{*}P < 0.017$ for significant mismatch: two-way ANOVA for each time (MRI measurements and groups) followed by paired *t*-test with Bonferroni correction. $^{\#}P < 0.008$ Fisher protected least significant difference for difference in mismatch volume between SHR ($n = 11$) and RH-WKY ($n = 7$) versus WKY ($n = 9$) following a significant ANOVA main group effect with no interaction. RH-WKY, renovascular-hypertensive WKY; SHR, spontaneously hypertensive rats; WKY, normotensive Wistar-Kyoto.

to those described in SHR (Barry *et al*, 1982). Nonetheless, and as discussed above, the intrinsic susceptibility of SHR to stroke independently from arterial hypertension may explain the exaggerated hypoperfusion seen at 240 minutes after occlusion in SHR relative to RH-WKY.

In RH-WKY, the ADC-defined lesion was also exacerbated compared with normotensive rats (Figure 4A). These data suggest that CAH is a major factor that accelerates the relapse of the penumbra into irreversibly damaged tissue. This argument is supported by the fact that a significant difference between the perfusion deficit and ADC-derived lesion (mismatch) was present in renovascular-hypertensive rats only at 30 minutes after the occlusion and then progressively disappeared (Figure 6). As RH-WKY and SHR manifested the same degree of hypertension, the differences in lesion size observed between RH-WKY and SHR after 2 hours of ischemia could be attributed to other factors independent of hypertension that take place in SHR.

In conclusion, our studies show that CAH, be it genetic or renovascular, shortens the duration of the ischemic penumbra and thus the window of therapeutic opportunity. The effects of efficient antihypertensive treatments on the spatiotemporal evolution of the penumbra need to be addressed. Are these therapies able to restore the extent of the ischemic penumbra and the efficiency of neuroprotective compounds? If yes, which hypertensive agent is optimal? In fact, antihypertensive therapies do not possess the same beneficial effect in the protection of end organ damage and decrease in the risk of stroke. Indeed, it is increasingly recognized that some antihypertensive therapies may have direct protective effects on the brain in parallel to the decrease in arterial pressure (Oprisiu-Fournier *et al*, 2009). Overall, the present data strongly support the necessity to integrate CAH in animal studies designed to test therapeutic interventions for stroke.

Disclosure/conflict of interest

The authors declare no conflict of interest.

References

Albers GW, Thijs VN, Wechsler L, Kemp S, Schlaug G, Skalabrin E, Bammer R, Kakuda W, Lansberg MG, Shuaib A, Coplin W, Hamilton S, Moseley M, Marks MP (2006) Magnetic resonance imaging profiles predict clinical response to early reperfusion: the diffusion and perfusion imaging evaluation for understanding stroke evolution (defuse) study. *Ann Neurol* 60:508–17

Bardutzky J, Shen Q, Henninger N, Bouley J, Duong TQ, Fisher M (2005) Differences in ischemic lesion evolution in different rat strains using diffusion and perfusion imaging. *Stroke* 36:2000–5

Barry DI, Strandgaard S, Graham DI, Braendstrup O, Svendsen UG, Vorstrup S, Hemmingsen R, Bolwig TG (1982) Cerebral blood flow in rats with renal and spontaneous hypertension: resetting of the lower limit of autoregulation. *J Cereb Blood Flow Metab* 2:347–53

Bråtane BT, Walvick RP, Corot C, Lancelot E, Fisher M (2010) Characterization of gadolinium-based dynamic susceptibility contrast perfusion measurements in permanent and transient MCAO models with volumetric based validation by CASL. *J Cereb Blood Flow Metab* 30:336–42

Del Bigio MR, Yan HJ, Kozlowski P, Sutherland GR, Peeling J (1999) Serial magnetic resonance imaging of rat brain after induction of renal hypertension. *Stroke* 30:2440–7

Durukan A, Strbian D, Tatlisumak T (2008) Rodent models of ischemic stroke: a useful tool for stroke drug development. *Curr Pharm Des* 14:359–70

Duverger D, MacKenzie ET (1988) The quantification of cerebral infarction following focal ischemia in the rat: influence of strain, arterial pressure, blood glucose concentration, and age. *J Cereb Blood Flow Metab* 8:449–61

Grandin CB, Duprez TP, Smith AM, Oppenheim C, Peeters A, Robert AR, Cosnard G (2002) Which MR-derived perfusion parameters are the best predictors of infarct growth in hyperacute stroke? Comparative study between relative and quantitative measurements. *Radiology* 223:361–70

Gratton JA, Sauter A, Rudin M, Lees KR, McColl J, Reid JL, Dominiczak AF, Macrae IM (1998) Susceptibility to cerebral infarction in the stroke-prone spontaneously hypertensive rat is inherited as a dominant trait. *Stroke* 29:690–4

Iadecola C, Davisson RL (2008) Hypertension and cerebrovascular dysfunction. *Cell Metab* 7:476–84

Kearney PM, Whelton M, Reynolds K, Muntner P, Whelton PK, He J (2005) Global burden of hypertension: analysis of worldwide data. *Lancet* 365:217–23

Lawes CMM, Vander Hoorn S, Rodgers A (2008) Global burden of blood-pressure-related disease, 2001. *Lancet* 371:1513–8

Lecrux C, Nicole O, Chazalviel L, Catone C, Chuquet J, MacKenzie ET, Touzani O (2007) Spontaneously hypertensive rats are highly vulnerable to AMPA-induced brain lesions. *Stroke* 38:3007–15

Legos JJ, Lenhard SC, Haimbach RE, Schaeffer TR, Bentley RG, McVey MJ, Chandra S, Irving EA, Andrew A Parsons, Barone FC (2008) SB 234551 selective ET(A) receptor antagonism: perfusion/diffusion MRI used to define treatable stroke model, time to treatment and mechanism of protection. *Exp Neurol* 212:53–62

Li JS, Knafo L, Turgeon A, Garcia R, Schiffrin EL (1996) Effect of endothelin antagonism on blood pressure and vascular structure in renovascular hypertensive rats. *Am J Physiol* 271:H88–93

Lin TN, He YY, Wu G, Khan M, Hsu CY (1993) Effect of brain edema on infarct volume in a focal cerebral ischemia model in rats. *Stroke* 24:117–21

Lövblad K, El-Koussy M, Oswald H, Baird AE, Schroth G, Mattle H (2003) Magnetic resonance imaging of the ischaemic penumbra. *Swiss Med Wkly* 133:551–9

McCabe C, Gallagher L, Gsell W, Graham D, Dominiczak AF, Macrae IM (2009) Differences in the evolution of the ischemic penumbra in stroke-prone spontaneously hypertensive and Wistar-Kyoto rats. *Stroke* 40:3864–8

Mulvany MJ, Hansen OK, Aalkjaer C (1978) Direct evidence that the greater contractility of resistance vessels in spontaneously hypertensive rats is associated with a narrowed lumen, a thickened media, and an increased number of smooth muscle cell layers. *Circ Res* 43:854–64

O'Collins VE, Macleod MR, Donnan GA, Horky LL, van der Worp BH, Howells DW (2006) 1,026 experimental treatments in acute stroke. *Ann Neurol* 59:467–77

Olivot JM, Marks MP (2008) Magnetic resonance imaging in the evaluation of acute stroke. *Top Magn Reson Imaging* 19:225–30

Oprisiu-Fournier R, Faure S, Mazouz H, Boutitie F, Serot J, Achard J, Godefroy O, Hanon O, Temmar M, Albu A, Strandgaard S, Wang J, Black SE, Fournier A (2009) Angiotensin AT1-receptor blockers and cerebrovascular protection: do they actually have a cutting edge over angiotensin-converting enzyme inhibitors? *Expert Rev Neurother* 9:1289–305

Schlaug G, Benfield A, Baird AE, Siewert B, Lövblad KO, Parker RA, Edelman RR, Warach S (1999) The ischemic penumbra: operationally defined by diffusion and perfusion MRI. *Neurology* 53:1528–37

Shen Q, Meng X, Fisher M, Sotak CH, Duong TQ (2003) Pixel-by-pixel spatiotemporal progression of focal ischemia derived using quantitative perfusion and diffusion imaging. *J Cereb Blood Flow Metab* 23:1479–88

Sobesky J, Zaro Weber O, Lehnhardt F, Hesselmann V, Neveling M, Jacobs A, Heiss W (2005) Does the mismatch match the penumbra? Magnetic resonance imaging and positron emission tomography in early ischemic stroke. *Stroke* 36:980–5

Stankevicius E, Martinez AC, Mulvany MJ, Simonsen U (2002) Blunted acetylcholine relaxation and nitric oxide release in arteries from renal hypertensive rats. *J Hypertens* 20:1571–9

Takaba H, Fukuda K, Yao H (2004) Substrain differences, gender, and age of spontaneously hypertensive rats critically determine infarct size produced by distal middle cerebral artery occlusion. *Cell Mol Neurobiol* 24:589–98

Takasawa M, Jones PS, Guadagno JV, Christensen S, Fryer TD, Harding S, Gillard JH, Williams GB, Aigbirhio FI, Warburton EA, Østergaard L, Baron J (2008) How reliable is perfusion MR in acute stroke? Validation and determination of the penumbra threshold against quantitative pet. *Stroke* 39:870–7

Thévenaz P, Ruttimann UE, Unser M (1998) A pyramid approach to subpixel registration based on intensity. *IEEE Trans Image Process* 7:27–41